

Photoresponsive Polymers and Block Copolymers by Molecular Recognition Based on Multiple Hydrogen Bonds

Alberto Concellón,¹ Eva Blasco,¹ Milagros Piñol,¹ Luis Oriol,¹ Isabel Díez,² Cristina Berges,² Carlos Sánchez-Somolinos,² Rafael Alcalá²

¹Departamento de Química Orgánica, Facultad de Ciencias, Instituto de Ciencia de Materiales de Aragón (ICMA), Universidad de Zaragoza-CSIC, 50009 Zaragoza, Spain

²Departamento de Física de la Materia Condensada, Facultad de Ciencias, Instituto de Ciencia de Materiales de Aragón (ICMA), Universidad de Zaragoza-CSIC, 50009 Zaragoza, Spain

Correspondence to: L. Oriol (E-mail: loriol@unizar.es)

Received 25 June 2014; accepted 5 August 2014; published online 00 Month 2014

DOI: 10.1002/pola.27373

ABSTRACT: A new methacrylate containing a 2,6-diacylamino-pyridine (DAP) group was synthesized and polymerized via RAFT polymerization to prepare homopolymethacrylates (PDAP) and diblock copolymers combined with a poly(methyl methacrylate) block (PMMA-*b*-PDAP). These polymers can be easily complexed with azobenzene chromophores having thymine (tAZO) or carboxylic groups with a dendritic structure (dAZO), which can form either three or two hydrogen bonds with the DAP groups, respectively. The supramolecular polymers were characterized by spectroscopic techniques, optical microscopy, TGA, and DSC. The supramolecular polymers and block copolymers with dAZO exhibited mesomorphic proper-

ties meanwhile with tAZO are amorphous materials. The response of the supramolecular polymers to irradiation with linearly polarized light was also investigated founding that stable optical anisotropy can be photoinduced in all the materials although higher values of birefringence and dichroism were obtained in polymers containing the dendrimeric chromophore dAZO. © 2014 Wiley Periodicals, Inc. *J. Polym. Sci., Part A: Polym. Chem.* **2014**, *00*, 000–000

KEYWORDS: azo polymers; block copolymers; hydrogen bonding; self-assembly; supramolecular polymers

INTRODUCTION In recent years, supramolecular chemistry has become an exciting field of research as a versatile approach to build up new dynamic functional materials based on self-assembly of complementary components,^{1–5} in particular because these self-assembled materials are easier to prepare when compared to entirely covalent systems, which usually require lengthy synthetic procedures. From the different interactions used to hold the molecular components together, H-bonding has been the most extensively used as a consequence of its directionality and selectivity.^{6,7} Among functional polymers, pioneering work on supramolecular liquid crystal polymers by Kato and Fréchet⁸ and Lehn and coworkers,⁹ has been followed by an increasing interest in these systems^{10,11} where a very common approach is based on macromolecules in which side chain mesogenic moieties are connected or built up by H-bonding.^{12–15}

The design of azobenzene photoaddressable polymers has traditionally focused on side-chain structures. These materials have been investigated as photomechanical actuators,^{16,17}

optical storage media,^{18–20} photoinduced chiral systems,²¹ photoresponsive surfaces,^{22,23} or light responsive nanocarriers,²⁴ among others. The basis of most reported applications is the reversible *trans-cis* photoisomerization experienced by the azobenzene unit. Furthermore, the rod-like structure of the azobenzene moieties is also the origin of the liquid crystalline properties reported for many of these azopolymers.^{25,26}

In our group, different series of azobenzene containing homopolymers and copolymers, mostly based on the covalent binding of chromophores to the main polymeric chain, have been described for different applications which include block copolymers for volume holographic storage.^{27–32} Along with the covalent one, supramolecular approaches based on the molecular recognition between chromophores and complementary side groups distributed along a polymeric chain have been less often considered.^{33–37} Very recently, we reported the preparation of a series of photoaddressable supramolecular polymers by mixing carboxy-terminated

Additional Supporting Information may be found in the online version of this article.

© 2014 Wiley Periodicals, Inc.

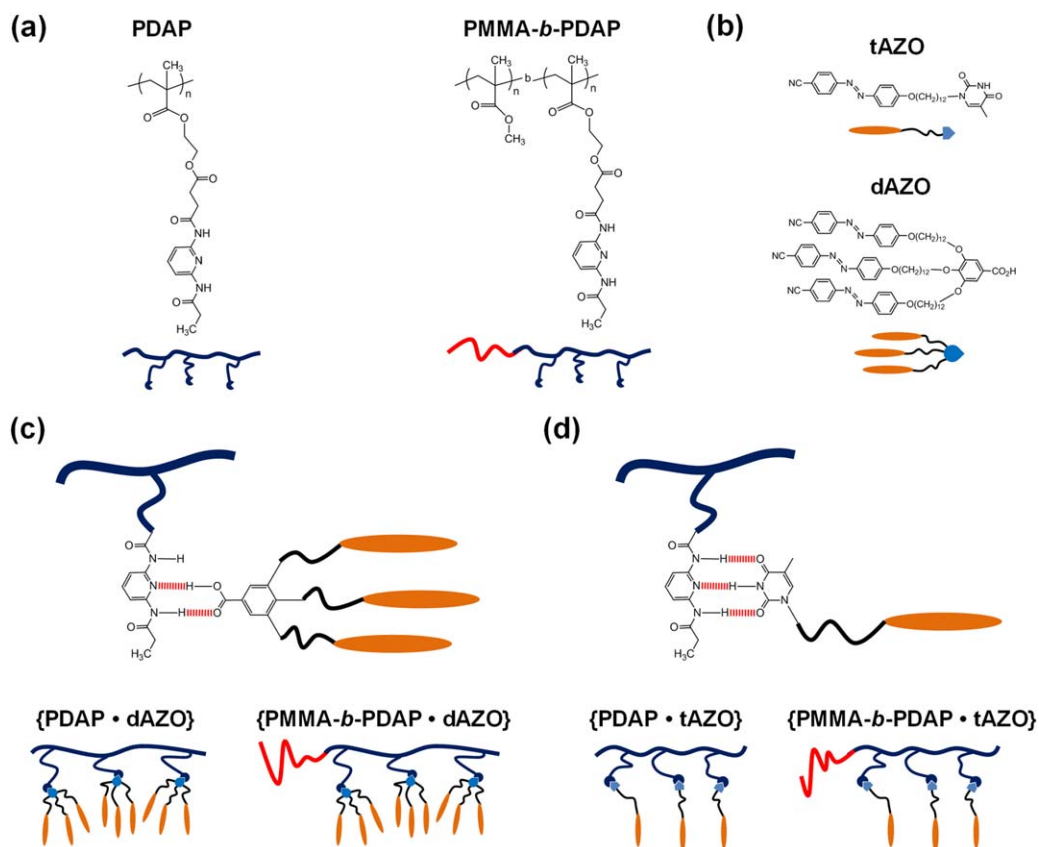


FIGURE 1 Chemical structures and schematic representations of (a) PDAP and PMMA-*b*-PDAP polymers, (b) dAZO and tAZO azobenzene chromophores, and (c) dAZO and (d) tAZO supramolecular complexes. [Color figure can be viewed in the online issue, which is available at wileyonlinelibrary.com.]

azobenzene derivatives and commercially available poly(4-vinylpyridine)s and polystyrene-*b*-poly(4-vinylpyridine) block copolymers, in which the promesogenic azobenzene chromophore was complexed to the polymer via H-bonding.^{38,39} Low complexation ratios (containing ≤ 50 molar % of the acid azo-derivatives), provided homogeneous liquid crystalline materials where interactions are formed through single-site H-bonding of the $-\text{COOH}$ groups of azobenzene moieties and the pyridyl groups of poly(4-vinylpyridine) chains. However, mixtures with higher molar ratios of the acids gave heterogeneous materials with evident signs of macrophase separation³⁸ which suggests that stronger H-bonding interactions are necessary if higher functionalized homogeneous materials are required. Viable option is to promote multiple H-bonding interactions as in DNA-like complexes. DNA has been an inspiration in polymer science and, as a consequence, the preparation of synthetic polymers that mimic DNA has been a challenge. During the last decades several studies reported the preparation of synthetic polymers having bases of nucleic acids as side groups or chain-ends.^{40–42} Following the approach, Rotello and coworkers reported nucleobase analogues containing polymers by incorporation of side-chain functionalities such as diaminotriazine and diacylaminopyridine.^{43–46}

In an attempt to get homogeneous photoaddressable materials with high degrees of azobenzene complexation via molec-

ular recognition, we report the synthesis of a series of polymers obtained from a methacrylic monomer containing a 2,6-diacylaminopyridine unit (monomer coded as **DAP**). The corresponding homopolymers (coded a **PDAP**), and diblock copolymers with poly (methyl methacrylate) (PMMA; coded as **PMMA-*b*-PDAP**) were complexed with azobenzene derivatives having a complementary thymine (**tAZO**) or carboxylic acid group (**dAZO**) to produce new azopolymers by H-bond self-assembly (Fig. 1). Compound **tAZO** contains a 4-cyanoazobenzene unit while **dAZO** has a dendritic structure with three 4-cyanoazobenzene units. By using a 1:1 molar ratio of the azocompound to the DAP repeating unit, fully complexed polymers were prepared to test if homogeneous materials can be obtained. In the case of the block copolymers, the PDAP block can selectively encapsulate the azo units whereas the PMMA block confers processability and transparency at the isomerization wavelength of the azobenzene chromophores. Thermal properties and microstructure, as well as the photoinduced anisotropy induced with linearly polarized light, were studied.

EXPERIMENTAL

Materials

Methyl methacrylate (Sigma-Aldrich, 99%) was passed through a basic alumina column, stored over CaH_2 , and

vacuum-distilled before use. 2,6-Diaminopyridine (Sigma-Aldrich, 98%) was recrystallized in ethanol before use. All other commercially available starting materials were purchased from Sigma-Aldrich and used as received without further purification. 3,4,5-Tris[12-(4-(4'-cyanophenyldiazo)phenoxy)dodecyloxy]benzoic acid (**dAZO**) was synthesized according to a previously described method.³⁹

Synthesis of Monomer DAP

2-Amino-6-propionylamidopyridine (**1**)

2,6-Diaminopyridine (12.5 g, 114.50 mmol) was dissolved in dry tetrahydrofuran (THF; 70 mL). A solution of propionyl chloride (5 mL, 57.60 mmol) in dry THF (10 mL) was added dropwise over more than 1 h to the solution of 2,6-diaminopyridine. The mixture was stirred for 3 h at RT. The precipitate was filtered off, and the solvent was evaporated. The crude product was recrystallized in ethanol/toluene (1:6). Yield: 77%. IR (KBr, ν , cm^{-1}): 3478, 3370, 3226, 1674, 1629, 1541, 1466, 793. ¹H NMR (CDCl_3 , 400 MHz, δ , ppm): 7.86 (s, 1H), 7.57–7.48 (m, 1H), 7.42 (dd, 1H, $J = 7.9$ Hz, $J = 7.9$ Hz), 6.23 (dd, 1H, $J = 7.9$ Hz, $J = 0.7$ Hz), 4.34 (s, 2H), 2.35 (q, 2H, $J = 7.5$ Hz), 1.19 (t, 3H, $J = 7.5$ Hz). ¹³C NMR (CDCl_3 , 100 MHz, δ , ppm): 172.3, 157.2, 150.0, 140.3, 104.3, 103.4, 30.8, 9.5.

2-(Propionylamino)-6-[4-(2-methacryloyloxy ethoxy)-4-oxobutanoylamino]pyridine (**DAP**)

4-(Dimethylamino) pyridinium *p*-toluene sulfonate (4.53 g, 14.53 mmol), 2-amino-6-propionylamidopyridine (**1**) (2.00 g, 12.11 mmol), and 4-[2-(methacryloyloxy)ethoxy]-4-oxobutanoic acid (3.35 g, 14.53 mmol) were dissolved in dry dichloromethane (15 mL). The reaction flask was cooled in an ice bath and flushed with argon, then *N,N'*-diisopropylcarbodiimide (1.83 g, 14.53 mmol) was added. The mixture was stirred at RT for 24 h under argon atmosphere. Then, the reaction was washed twice with water and once with brine. Finally, the organic layer was dried over anhydrous magnesium sulfate and the solvent was evaporated. The crude product was purified by flash column chromatography on silica gel using hexane/ethyl acetate (1:1) as eluent. Then the product was recrystallized in ethanol. Yield: 64%. IR (KBr, ν , cm^{-1}): 3336, 1724, 1690, 1639, 1586, 1512, 1453, 1316, 1152, 805. ¹H NMR (CDCl_3 , 400 MHz, δ , ppm): 8.10–7.60 (m, 5H), 6.14–6.09 (m, 1H), 5.60–5.53 (m, 1H), 4.44–4.30 (m, 4H), 2.85–2.74 (m, 2H), 2.72–2.63 (m, 2H), 2.43 (q, 2H, $J = 7.5$ Hz), 1.98–1.88 (m, 3H), 1.24 (t, 3H, $J = 7.5$ Hz). ¹³C NMR (CDCl_3 , 100 MHz, δ , ppm): 172.6, 172.5, 167.4, 149.8, 149.3, 140.9, 136.0, 126.4, 109.6, 109.5, 62.7, 62.5, 32.3, 30.8, 29.4, 18.4, 9.5. MS (MALDI⁺, dithranol, m/z): calcd for $\text{C}_{18}\text{H}_{23}\text{N}_3\text{O}_6$, 377.16; found, 378.17 $[\text{M} + \text{H}]^+$, 400.15 $[\text{M} + \text{Na}]^+$. Anal. calcd for $\text{C}_{18}\text{H}_{23}\text{N}_3\text{O}_6$: C, 57.29%; H, 6.14%; N, 11.13%. Found: C, 57.32%; H, 6.31%; N, 11.20%.

Synthesis of Azocompounds

4-Cyano-4'-(12''-bromododecyloxy) azobenzene (see Scheme S1 in Supporting Information, Compound 2)

A solution of 4-cyano-4'-hydroxyazobenzene (3.00 g, 13.43 mmol) in acetone (50 mL) was added dropwise over more than 1 h to a mixture of 1,12-dibromododecane (5.30 g,

16.12 mmol), potassium carbonate (3.71 g, 26.86 mmol), 18-crown-6 (0.28 g, 1.07 mmol) in acetone (10 mL). Then it was stirred and heated to reflux for 12 h. The reaction was allowed to cool down to RT and the solids filtered off and washed with acetone. The solvent was evaporated under reduced pressure and the residue was purified by flash column chromatography using hexane/dichloromethane (1:1) as eluent. Yield: 67%. IR (KBr, ν , cm^{-1}): 2223, 1600, 1498, 1466, 1257, 1138, 840, 560. ¹H NMR (CDCl_3 , 400 MHz, δ , ppm): 7.99–7.90 (m, 4H), 7.85–7.75 (m, 2H), 7.05–6.98 (m, 2H), 4.06 (t, 2H, $J = 6.5$ Hz), 3.41 (t, 2H, $J = 6.9$ Hz), 1.92–1.77 (m, 4H), 1.52–1.21 (m, 16H). ¹³C NMR (CDCl_3 , 100 MHz, δ , ppm): 162.9, 155.0, 146.9, 133.3, 125.6, 123.2, 118.8, 115.0, 113.3, 68.6, 34.2, 33.0, 29.7, 28.8, 28.3, 26.1.

N(1)-[12-(4-(4'-cyanophenyldiazo)phenoxy)dodecyloxy]thymine (**tAZO**)

4-Cyano-4'-(12''-bromododecyloxy)azobenzene (3 g, 6.38 mmol), thymine (2.41 g, 19.13 mmol), and potassium carbonate (2.64 g, 19.13 mmol) in dimethyl sulfoxide (250 mL) were stirred and heated at 60 °C for 12 h. Then, the reaction was poured into 150 mL of ethyl acetate, washed twice with water and twice with brine. Finally, the organic layer was dried over anhydrous magnesium sulfate. The solvent was distilled off giving an orange solid that was purified by flash column chromatography on silica gel using hexane/ethyl acetate (2:1) as eluent. Yield: 27%. IR (KBr, ν , cm^{-1}): 3162, 3041, 2229, 1696, 1601, 1582, 1501, 1470, 1250, 1142, 853. ¹H NMR (CDCl_3 , 400 MHz, δ , ppm): 8.45 (s, 1H), 7.99–7.88 (m, 4H), 7.82–7.75 (m, 2H), 7.05–6.92 (m, 3H), 4.05 (t, 2H, $J = 6.5$ Hz), 3.73–3.63 (m, 2H), 1.92 (t, 3H, $J = 1.8$ Hz), 1.87–1.77 (m, 2H), 1.72–1.57 (m, 2H), 1.54–1.21 (m, 16H). ¹³C NMR (CDCl_3 , 100 MHz, δ , ppm): 164.2, 162.9, 155.0, 150.8, 146.8, 140.5, 133.3, 125.6, 123.2, 118.8, 115.0, 113.3, 110.6, 68.6, 48.7, 29.7–29.1, 26.6, 26.1, 12.5. MS (MALDI⁺, dithranol, m/z): calcd for $\text{C}_{30}\text{H}_{37}\text{N}_5\text{O}_3$, 515.29; found, 516.29 $[\text{M} + \text{H}]^+$, 538.29 $[\text{M} + \text{Na}]^+$. Anal. calcd for $\text{C}_{30}\text{H}_{37}\text{N}_5\text{O}_3$: C, 69.88%; H, 7.23%; N, 13.58%. Found: C, 69.66%; H, 7.10%; N, 13.59%.

Synthesis of Polymers

Homopolymers PDAP_A and PDAP_B

The monomer **DAP** (1.0 g, 2.65 mmol), 4-cyano-4-(phenylcarbonothioylthio)pentanoic acid (for PDAP_A: 14.0 mg, 0.05 mmol; for PDAP_B: 7.0 mg, 0.025 mmol), 2,2'-azobisisobutyronitrile (AIBN; for PDAP_A: 2.0 mg, 0.012 mmol; for PDAP_B: 1.0 mg, 0.006 mmol), and DMF as solvent (3 mL) were added to a Schlenk flask closed with a rubber septum. The flask was deoxygenated by three freeze-pump-thaw cycles and flushed with argon. The reaction mixture was stirred at 80 °C. After 48 h, the mixture was quenched with liquid nitrogen and diluted with THF, and then it was carefully precipitated using cold methanol. The polymer was dried in a vacuum oven at 40 °C for 24 h. Yield: 71% (for PDAP_A) and 88% (for PDAP_B).

Characterization Data of PDAP_A

IR (KBr, ν , cm^{-1}): 3333, 1736, 1700, 1586, 1516, 1450, 1293, 1152, 803. ¹H NMR (CDCl_3 , 400 MHz, δ , ppm):

9.08–8.30 (m, 2H), 7.98–7.48 (m, 3H), 4.50–3.86 (m, 4H), 2.98–2.52 (m, 4H), 2.49–2.25 (m, 2H), 2.02–1.60 (m, 2H), 1.47–0.64 (m, 6H), 1.47–0.64 (m, 6H). Anal. calcd for $C_{18}H_{23}N_3O_6$: 57.29%; H, 6.14%; N, 11.13%. Found: C, 56.16%; H, 6.38%; N, 10.88%; S, 0.34%.

Characterization Data of PDAP_B

IR (KBr) ν (cm^{-1}): 3331, 1737, 1700, 1586, 1512, 1449, 1293, 1151, 803. 1H NMR ($CDCl_3$, 400 MHz) δ (ppm): 9.05–8.32 (m, 2H), 8.00–7.46 (m, 3H), 4.52–3.84 (m, 4H), 3.06–2.58 (m, 4H), 2.54–2.25 (m, 2H), 2.02–1.60 (m, 2H), 1.46–0.63 (m, 6H). Anal. calcd for $C_{18}H_{23}N_3O_6$: 57.29%; H, 6.14%; N, 11.13%. Found: C, 56.16%; H, 6.48%; N, 11.14%; S, 0.23%.

PMMA-CTA for RAFT Polymerization

Methyl methacrylate (7.5 mL, 70.12 mmol), 4-cyano-4-(phenylcarbonothioylthio)pentanoic acid (32.7 mg, 0.234 mmol), AIBN (3.85 mg, 0.047 mmol), and toluene (2.5 mL) were added to a Schlenk flask closed with a rubber septum. The flask was deoxygenated by three freeze-pump-thaw cycles and flushed with argon. The reaction mixture was stirred at 60 °C. After 12 h the mixture was quenched with liquid nitrogen and diluted with THF, and then it was carefully precipitated using cold methanol. The polymer was dried in a vacuum oven at 40 °C for 24 h. Yield: 82%. IR (KBr) ν (cm^{-1}): 1731, 1244, 1149. 1H NMR ($CDCl_3$, 400 MHz) δ (ppm): 3.71–3.37 (s, 3H), 2.10–0.62 (m, 5H). Anal. calcd for $C_5H_8O_2$: C, 59.98%; H, 8.05%. Found: C, 59.81%; H, 8.79%; N, 0.53%; S, 0.50%.

Block Copolymers PMMA-*b*-PDAP_C and PMMA-*b*-PDAP_D

DAP (0.5 g, 1.33 mmol), PMMA-CTA (for PMMA-*b*-PDAP_C: 1.37 g, 0.025 mmol; for PMMA-*b*-PDAP_D: 0.68 g, 0.012 mmol), AIBN (for PMMA-*b*-PDAP_C: 1.0 mg, 0.006 mmol; for PMMA-*b*-PDAP_D: 0.5 mg, 0.003 mmol) and DMF (for PMMA-*b*-PDAP_C: 5 mL; for PMMA-*b*-PDAP_D: 3 mL) were added to a Schlenk flask closed with a rubber septum. The flask was deoxygenated by three freeze-pump-thaw cycles and flushed with argon. The reaction mixture was stirred at 80 °C. After 48 h the mixture was quenched with liquid nitrogen, and then it was carefully precipitated using cold methanol. The polymer was dried in a vacuum oven at 40 °C for 24 h. Yield: 82% (for PMMA-*b*-PDAP_C) and 68% (for PMMA-*b*-PDAP_D).

Characterization Data of PMMA-*b*-PDAP_C

IR (KBr) ν (cm^{-1}): 3340, 1734, 1588, 1452, 1244, 1147. 1H NMR ($CDCl_3$, 400 MHz) δ (ppm): 8.86–8.44 (m, 2H), 7.93–7.50 (m, 3H), 4.39–3.92 (m, 4H), 3.68–3.43 (m, 4H), 2.89–2.61 (m, 4H), 2.46–2.31 (m, 2H), 2.15–0.69 (m, 115H). Anal. calcd for $C_{3398}H_{5228}N_{108}O_{1316}$: 59.45%; H, 7.68%; N, 2.20%. Found: C, 59.00%; H, 8.04%; N, 2.47%; S, 0.28%.

Characterization Data of PMMA-*b*-PDAP_D

IR (KBr) ν (cm^{-1}): 3337, 1733, 1588, 1452, 1243, 1149. 1H NMR ($CDCl_3$, 400 MHz) δ (ppm): 8.90–8.43 (m, 2H), 7.99–7.44 (m, 3H), 4.46–3.86 (m, 4H), 3.66–3.49 (m, 20H),

2.93–2.54 (m, 4H), 2.46–2.22 (m, 2H), 2.14–0.61 (m, 43H). Anal. calcd for $C_{4262}H_{6332}N_{252}O_{1604}$: 59.00%; H, 7.36%; N, 4.07%. Found: C, 58.52%; H, 7.64%; N, 4.14%; S, 0.31%.

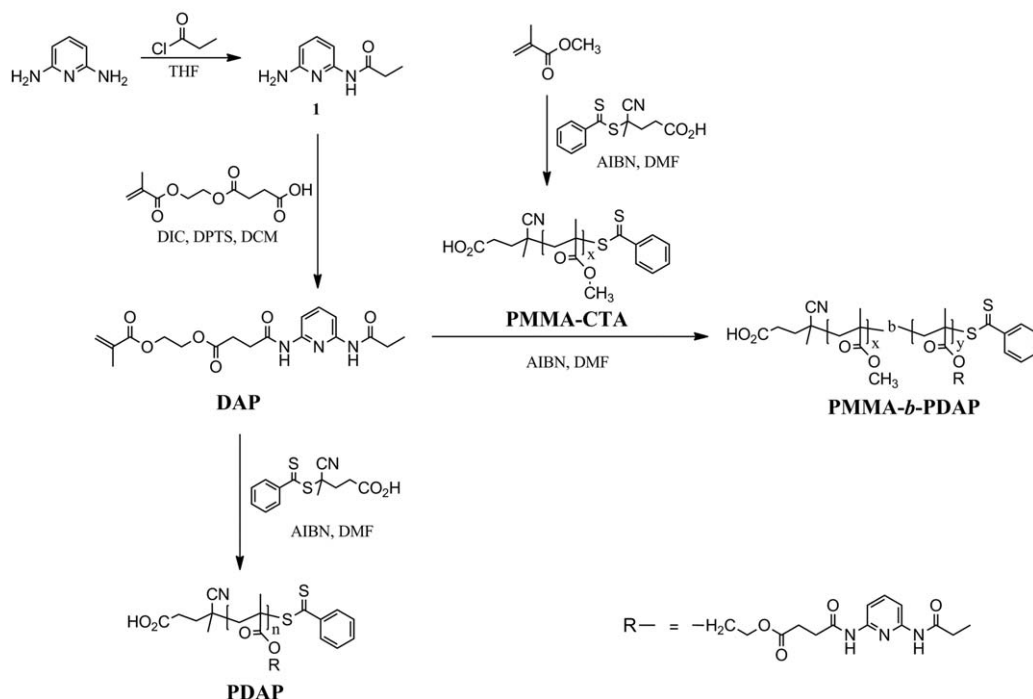
Supramolecular Polymers Preparation

The required amounts of polymer and azobenzene chromophores were weighed and dissolved in THF followed by stirring overnight at room temperature. Finally, the solvent was slowly evaporated and the mixtures were dried under vacuum at 40 °C for at least 2 days.

Characterization Techniques

IR spectra were obtained on a Bruker Vertex 70 FT-IR spectrophotometer. NMR spectra were recorded on a Bruker AV-400 spectrometer. Elemental analysis was performed using a Perkin-Elmer 2400 microanalyzer. MALDI-TOF MS was performed on an Autoflex mass spectrometer (Bruker Daltonics) using dithranol as matrix. Size exclusion chromatography (SEC) was carried out on a Waters e2695 Alliance liquid chromatography system equipped with a Waters 2424 evaporation light scattering detector and a Waters 2998 PDA detector using two Styragel columns, HR4 and HR1 from Waters. Measurements were performed in THF with a flow of 1 mL min^{-1} using PMMA narrow molecular weight standards. SEC measurements for PDAP homopolymers were carried out in DMF with LiBr (50 mM) with a flow of 0.5 mL min^{-1} to avoid aggregation effects observed in THF; in this case polystyrene (PS) narrow molecular weight standards were used with the UV-PDA detector. Thermogravimetric analysis (TGA) was performed using a TA Q5000IR instrument at heating rate of 10 °C min^{-1} under a nitrogen atmosphere. Mesogenic behavior was investigated by polarized-light optical microscopy (POM) using a Olympus BH-2 polarizing microscope fitted with a Linkam THMS600 hot stage. Thermal transitions were determined by differential scanning calorimetry (DSC) using a TA DSC Q-2000 instrument under nitrogen atmosphere with powdered samples (2–5 mg) sealed in aluminum pans. Glass transition temperatures (T_g) were determined at the half height of the baseline jump, and the mesophase-to-isotropic phase transition temperatures were read at the maximum of the corresponding peaks. X-ray diffraction (XRD) were performed with an evacuated Pinhole camera (Anton-Paar) operating a point-focused Ni-filtered Cu- K_α beam. The patterns were collected on flat photographic films perpendicular to the X-ray beam. Powdered samples of the supramolecular complexes were placed into quartz Lindemann capillaries (1 mm diameter).

Samples for transmission electron microscopy (TEM) measurements were prepared as follows. A few milligrams of each material were molded to form a pellet, the samples were then heated at 150 °C and quenched to room temperature. After this process, ultrathin sections of about 100 nm were obtained using a Leica ultramicrotome equipped with a diamond knife, and picked up on carbon-coated copper grids. To enhance the contrast, the grids were exposed to ruthenium oxide (RuO_4) vapor for 1 h. The staining agent was purchased from PolySciences and used without further



SCHEME 1 Synthesis of DAP monomer, PDAP homopolymers, and PMMA-*b*-PDAP block polymers.

purification. TEM was measured using a Tecnai T20 electron microscope operating at 200 kV.

Film thickness was measured a DEKTAK profilometer. For optical absorption and dichroism experiments, a Varian Cary 500 UV-vis-NIR spectrophotometer was used. For dichroism measurements, a linear polarizer was placed before the film.

RESULTS AND DISCUSSION

Synthesis and Characterization of Building Blocks

The polymeric precursors of the supramolecular polymers were prepared from the monomer **DAP**, which was obtained through a nonsymmetric two-steps amidation of 2,6-diaminopyridine moiety (Scheme 1). The first step was a monoacylation of 2,6-diaminopyridine with propionyl chloride⁴⁷ and the second step involved an amidation with 4-[2-(methacryloyloxy) ethoxy]-4-oxobutanoic acid to introduce the methacrylic polymerizable group. Monomer **DAP** was purified by flash column chromatography and subsequent recrystallization and adequately characterized by FTIR, NMR (see Fig. S1 in Supporting Information), MALDI-TOF MS, and elemental analysis.

Two homopolymers and two diblock copolymers were prepared by reversible addition–fragmentation chain transfer (RAFT) polymerization.^{48,49} PDAP homopolymers were obtained using the RAFT agent 4-cyano-4-(phenylcarbonothioylthio)pentanoic acid (Scheme 1) and adjusting the monomer to RAFT agent molar ratios to obtain two different molar masses. The SEC curves showed monomodal molar mass distributions with low polydispersity values, $D_M < 1.2$. The relative average number molar masses estimated by SEC

using polymer standards (M_n^{SEC}) are gathered in Table 1. Calculation of average molar masses of PDAP homopolymers was not possible by ¹H NMR (M_n^{NMR}) as end-groups were not detected by this technique.

Diblock copolymers can be obtained by two sequential RAFT polymerizations, firstly preparing a thiocarbonylthio-terminated prepolymer that is subsequently used as a macro-RAFT agent in a second polymerization step. In the synthesis of PMMA-*b*-PDAP diblock copolymers, a PMMA block was first prepared and used as macro-RAFT agent (**PMMA-CTA**) (Scheme 1). The molar mass of this PMMA was determined by SEC using PMMA standards. Then, two diblock copolymers were prepared by adjusting the monomer **DAP** to **PMMA-CTA** molar ratios to get different degree

TABLE 1 Molar Mass and Molar Mass Distributions of the Synthesized Polymers

Polymer	M_n^{NMR}	M_n^{SEC}	D_M
PDAP _A	–	60,900 ^a	1.19 ^a
PDAP _B	–	73,400 ^a	1.15 ^a
PMMA-CTA	–	55,000 ^b	1.02 ^b
PMMA- <i>b</i> -PDAP _C	68,600 ^c	67,600 ^b	1.04 ^b
PMMA- <i>b</i> -PDAP _D	86,700 ^c	88,800 ^b	1.09 ^b

^a M_n^{SEC} and D_M were calculated by SEC using DMF (LiBr 50 mM; 0.5 mL min⁻¹) as the mobile phase relative to PS standards.

^b M_n^{SEC} and D_M were calculated by SEC using THF (1 mL min⁻¹) as the mobile phase relative to PMMA standards.

^c M_n^{NMR} were calculated by comparing NMR integrated signals of repeating units of both blocks and using the molar mass of PMMA block measured by SEC (using PMMA standards).

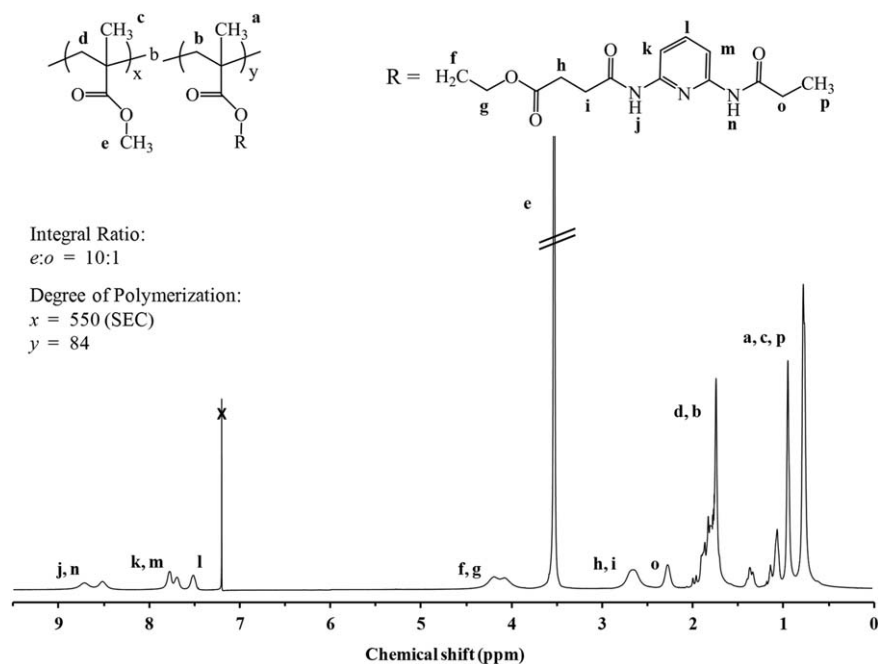


FIGURE 2 ^1H NMR spectrum (400 MHz, CDCl_3) recorded for PMMA-*b*-PDAP_D. The degree of polymerization of the PDAP block (y) was calculated from the relative integration of signals e and o , taking for the PMMA block $x = 550$, which is the value determined by SEC using PMMA standards (see text).

of polymerization of the PDAP block. This time, ^1H NMR spectroscopy was employed to calculate average molar masses (M_n^{NMR} in Table 1) of the block copolymers by relative integration of the PMMA methyl proton signals ($\text{O}-\text{CH}_3$, coded as e in Fig. 2) and the corresponding ones to the methylene protons of PDAP block ($\text{CH}_3-\text{CH}_2-\text{CO}$, coded as o in Fig. 2) and taken as reference the M_n value determined by SEC for PMMA-CTA (M_n^{SEC}). SEC curves of PMMA-*b*-PDAP showed monomodal molar mass distributions with low polydispersities ($\mathcal{D}_M < 1.1$) and residual block precursors were not detected (see Fig. S5 in Supporting Information). M_n values estimated by SEC were in good agreement with those calculated by ^1H NMR.

Thermal analysis of the polymers was undertaken by TGA and DSC, and results are collected in Table 2. In the thermogravimetric study, degradation associated to weight loss was observed above 230 °C for all the synthesized polymeric precursors. All these polymers were amorphous materials as determined from the DSC curves where clear baseline jumps corresponding to the glass transitions were only observed. PDAP homopolymers exhibited a T_g around 75 °C. Diblock copolymers showed two glass transitions, which points to a microphase separation of both amorphous blocks. The lowest T_g corresponds to the PDAP block while the highest one is assigned to the PMMA block.

Two different photochromic azobenzene derivatives were used for complexation with the described polymers, **dAZO** and **tAZO**. The azodendrimer **dAZO** was obtained following a previously described synthetic approach.³⁹ **tAZO** was synthesized in two steps; first by alkylation of 4-cyano-4'-

hydroxyazobenzene with 1,12-dibromododecane under standard Williamson conditions, and second by a nucleophilic substitution with thymine (see Scheme S1 in Supporting Information). Both compounds showed onsets of decomposition at temperatures higher than 300 °C in the thermogravimetric study (Table 2). The thermal and mesomorphic properties of the azocompounds were studied by POM and DSC (Table 2). **tAZO** was a crystalline material that melted to give an isotropic liquid phase. However, **dAZO** exhibited a monotropic smectic A (SmA) liquid crystalline phase, with a melting transition at 150 °C and an isotropic-to-mesophase transition at 138 °C. The SmA mesophase was characterized by fan-shaped textures and a latent heat value at the I-SmA transition of $\Delta H_{\text{I-SmA}} = 13 \text{ kJ mol}^{-1}$, which is in accordance with previously described results.³⁹

Preparation and Characterization of PDAP and PMMA-*b*-PDAP Supramolecular Complexes

The supramolecular polymeric materials were prepared by dissolving the corresponding amount of the polymer (PDAP_A, PDAP_B, PMMA-*b*-PDAP_C, or PMMA-*b*-PDAP_D) and the azo chromophore (**dAZO** or **tAZO**) in THF, followed by stirring and slow evaporation of the solvent. The amount of chromophore was calculated to complex all the DAP moieties. For comparison purposes, all the mixtures were heated at 150 °C for 5 min and then rapidly quenched to room temperature. The mixtures obtained in this way appeared as homogeneous materials, providing evidence for the formation of an H-bonded complex. To confirm the existence of H-bonding interactions between DAP derivative units and **tAZO** or

TABLE 2 Thermal Parameters Obtained for the Precursors and Supramolecular Polymers

Compound	$T_{\text{onset}}^{\text{a}}$ (°C)	$T_{\text{g},1}^{\text{b}}$ (°C)	$T_{\text{g},2}^{\text{b}}$ (°C)	T_{m}^{c} (°C) [$\Delta H_{\text{m}}/\text{az.u.}$]	$T_{\text{I-M}}^{\text{c}}$ (°C) [$\Delta H_{\text{I-M}}/\text{az.u.}$]	T_{c}^{c} (°C) [$\Delta H_{\text{c}}/\text{az.u.}$]	$w_{\text{PDAP}}^{\text{d}}$	Chromophore ^e (wt %)
PDAP _A	245	75	–	–	–	–	1	–
PDAP _B	255	73	–	–	–	–	1	–
PMMA-CTA	320	–	123	–	–	–	0	–
PMMA- <i>b</i> -PDAP _C	235 ^f	83	118	–	–	–	0.20	–
PMMA- <i>b</i> -PDAP _D	240	82	119	–	–	–	0.37	–
tAZO	340	–	–	153 [13.4]	–	90 [32.3]	0	43
{PDAP _A • tAZO}	280	49	–	–	–	–	1	25
{PDAP _B • tAZO}	280	51	–	–	–	–	1	25
{PMMA- <i>b</i> -PDAP _C • tAZO}	290	60	113	–	–	–	0.37	9
{PMMA- <i>b</i> -PDAP _D • tAZO}	280	54	109	–	–	–	0.58	15
dAZO	345	–	–	150 [35.0]	138 [4.3]	89 [23.4]	0	50
{PDAP _A • dAZO}	235	36	–	146 [28.6]	125 [3.6]	74 [18.7]	1	39
{PDAP _B • dAZO}	255	38	–	145 [25.7]	124 [3.6]	69 [18.2]	1	39
{PMMA- <i>b</i> -PDAP _C • dAZO}	250	34	107	146 [27.0]	127 [4.3]	75 [16.4]	0.53	20
{PMMA- <i>b</i> -PDAP _D • dAZO}	260	34	108	145 [29.3]	125 [4.2]	70 [19.4]	0.72	29

^a Onset of the decomposition detected in the thermogravimetric curve.

^b Glass transition determined by DSC from the second heating scan (scan rate: 10 °C min⁻¹): $T_{\text{g},1}$ corresponds to PDAP and $T_{\text{g},2}$ to PMMA.

^c T_{m} : melting temperature read at the maximum of the peak (second heating). $T_{\text{I-M}}$: isotropic-to-mesophase temperature read at the minimum of the peak (second cooling). T_{c} : crystallization temperature read

at the minimum of the peak (second cooling). $\Delta H/\text{az.u.}$: enthalpy normalized by mol of azobenzene unit in kJ mol⁻¹.

^d Mass fraction of PDAP block (complexed with dAZO or tAZO in case of supramolecular complexes).

^e Weight percentage of chromophoric units (4-oxy-4'-cyanoazobenzene).

^f A small weight loss was detected at 165 °C associated to the presence of volatile compounds.

dAZO, FTIR spectroscopic studies were carried out using polymer films deposited onto KBr pellets.

On complexing with **tAZO**, the IR spectra of the supramolecular homopolymers or copolymers recorded for the just evaporated and the thermal annealed samples are very similar (see Fig. S6 in Supporting Information). Because the 2,6-diaminopyridine repeating unit can form three H-bonds with the thymine group, preparation of the supramolecular polymers by mixing in solution and evaporation probably leads to an essentially stable and homogeneous system and, for this reason, thermal treatment did not cause any significant changes in the IR spectra. In these polymers, complexation induced a decrease of the wavenumber of the N–H *st.* vibration band of DAP unit indicating the H-bond formation with the photochromic units containing thymine groups [Fig. 3(a)]. In the C=O *st.* region, a decrease of around 5–10 cm⁻¹ in the wavenumber of the C=O *st.* vibration of thymine group (1696 cm⁻¹) after complexation also supported the H-bonding interactions between complementary **tAZO** and DAP repeating units [Fig. 3(b)].

In the case of supramolecular homopolymers containing **dAZO**, where the DAP unit can form two H-bonds with the carboxylic acid, the thermal annealing at 150 °C was accompanied by significant changes in different regions of the IR spectra. The thermal treatment induced a shift to lower wavenumber of the N–H *st.* vibration due to the association

of DAP groups and **dAZO** [Fig. 4(a)]. Also the C=O *st.* region [Fig. 4(b)] suffered, after thermal treatment, an absorbance decrease of the peak at 1730 cm⁻¹ and an increase of the peak at 1685 cm⁻¹, most probably due to H-bonding interactions with the DAP core. The carbonyl stretching band in carboxylic acids usually appears at 1730 or 1685 cm⁻¹ for free or associated carbonyl groups, respectively. After thermal treatment, 1730 cm⁻¹ band did not completely disappear because it comprises contributions from the polymer ester groups. These changes reveal that the thermal annealing is required for a good homogenization. In a similar way, thermal treatment of **dAZO** containing supramolecular diblock copolymers induced a decrease of the wavenumber of the N–H *st.* vibration (see Fig. S8 in Supporting Information). In addition, after thermal treatment the band at 1685 cm⁻¹ (C=O *st.* region) was clearly detected. All these changes, which are similar for the homopolymer-based complexes, were attributed to H-bonding interactions between complementary **dAZO** and DAP repeating units.

Thermal Characterization of Supramolecular Complexes

The thermogravimetric study of the supramolecular complexes revealed that weight losses associated to the presence of residual solvents or water were not detected and all materials showed good thermal stability up to around 250 °C (Table 2). The thermal transitions and mesomorphic properties were studied by POM and DSC and the results are

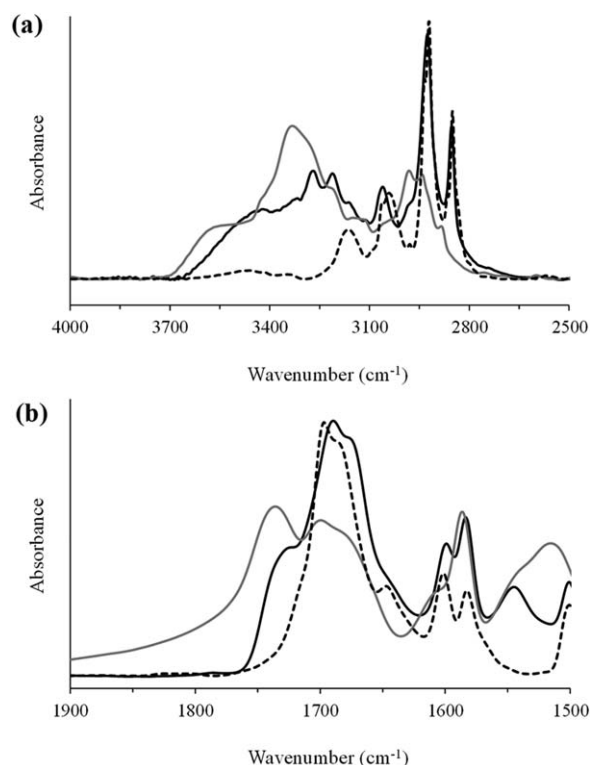


FIGURE 3 FTIR spectra of {PDAP_B • tAZO} (black), PDAP_B (gray), and tAZO (dash) as obtained (no significant variations were observed after thermal annealing): (a) N–H *st.* and (b) C=O *st.* region. (See Supporting Information for the spectra of the corresponding block copolymers).

gathered in Table 2. It should be mentioned that all the supramolecular polymers appeared as homogeneous materials by POM in heating-cooling cycles. In the case of dAZO complexes, the study of the samples was carried out after annealing at 150 °C. Segregation of the components was not observed for any of the complexes, which seems to indicate the formation of a single material through H-bonding interactions.

Supramolecular homopolymers containing tAZO were amorphous materials, DSC curves showed a baseline jump corresponding to the glass transition (Fig. 5). Glass transition of these supramolecular complexes was detected around 50 °C and was lower than that of the corresponding PDAP polymeric precursor. This fact can be attributed to a plasticization effect of the pendant tAZO moieties hydrogen bonded to the polymer. In the case of block copolymers containing tAZO, DSC curves showed two glass transitions agreeing with the constituent amorphous blocks, PMMA and the complexed PDAP blocks (Fig. 5). The presence of the two glass transitions seems to evidence the typical microphase segregation of block copolymers with a confinement of the azobenzene chromophores in the nanodomains of PDAP blocks.

In contrast to tAZO, the dendritic azobenzene derivative dAZO gave rise to mesomorphic materials. Supporting Infor-

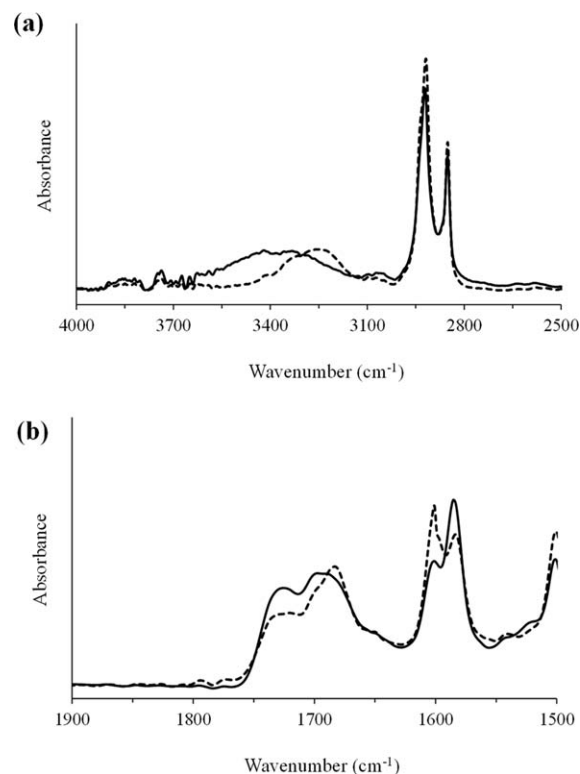


FIGURE 4 FTIR spectra of {PDAP_B • dAZO} before (solid) and after (dash) thermal annealing at 150 °C, 5 min: (a) N–H *st.* and (b) C=O *st.* region. (See Supporting Information for the spectra of the corresponding block copolymers).

mation Figure S9 displays a typical smectic texture observed by POM for dAZO-containing supramolecular homopolymers when was cooled down from the isotropic state (dAZO-complexed block copolymers exhibited less defined smectic textures as it is observed in Figure S10, Supporting Information). This monotropic liquid crystal phase was exhibited in a temperature range similar to that of the chromophore precursor dAZO. Thermal transition temperatures and enthalpy values for these complexes were investigated

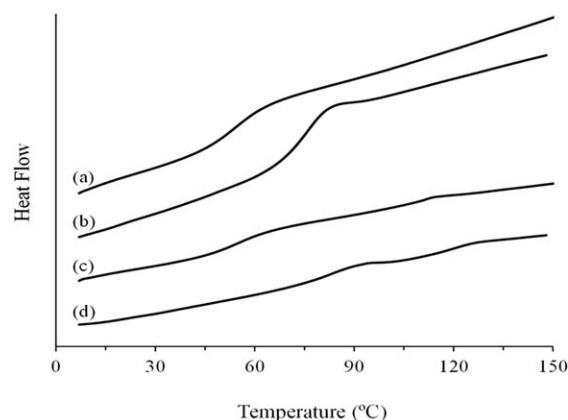


FIGURE 5 DSC traces of: (a) {PDAP_B • tAZO}, (b) PDAP_B, (c) {PMMA-*b*-PDAP_D • tAZO}, and (d) PMMA-*b*-PDAP_D corresponding to the second heating scan (10 °C min⁻¹; Exo down).

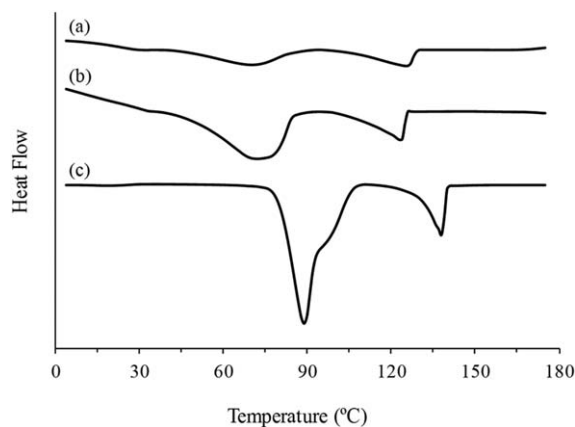


FIGURE 6 DSC traces of: (a) {PMMA-*b*-PDAP_D • dAZO}, (b) {PDAP_B • dAZO}, and (d) dAZO corresponding to the second cooling scan (10 °C min⁻¹; Exo down).

by DSC (Fig. 6 and Table 2). It can be observed that $\Delta H/az.u.$ (enthalpies normalized per mol of azobenzene unit) were similar to that of neat **dAZO**, therefore mesophase stability is not highly affected by complexing **dAZO** with a nonliquid crystal material. To characterize the structural parameters of mesophase, XRD studies were carried out. At low angles the first-order reflection of the smectic layers was detected at around 42 Å for samples rapidly cooled from the isotropic state to RT (Supporting Information Fig. S9). In addition, a diffuse halo was also detected in the 4–5 Å range which is typically associated to molecules in a short range distance correlation. The molecular length of **dAZO** estimated with

Dreiding stereomodels for its fully extended conformations is 36 Å and for the DAP repeating unit is 5 Å. Since the calculated length of **dAZO** plus the DAP repeating unit is comparable to the experimentally obtained smectic spacing, a monolayer structure is a reasonable model for the SmA mesophase of the complexed polymers. The measured smectic spacing was similar for all polymers regardless of the molecular weight and the structure (homo or block copolymer structure) of the polymers.

The supramolecular complexes of PMMA-*b*-PDAP block polymers complexed with **dAZO** chromophores can lead to materials with two hierarchical self-assembly levels: (a) the liquid crystalline organization of the chromophores within the PDAP domains and (b) the phase separated structures because of segregation between the PMMA and PDAP forming hydrogen bonds with **dAZO** blocks.^{50,51} In fact, the appearance of several thermal events in DSC ascribable to the different blocks already suggested phase segregation in these materials. It is well known that diblock copolymers are able to undergo microphase separation in the solid state leading to different morphologies such as spheres, cylinders or lamellae. This microphase separation depends on several parameters and in particular on the volume fraction of the blocks.^{52,53} We have studied the phase segregation of the parent diblock copolymers as well as their corresponding supramolecular complexes by TEM. As described in the Experimental section, the samples were annealed at 150 °C and then quenched to room temperature. **PMMA-*b*-PDAP_C** showed a weakly phase segregated morphology [Fig. 7(a)], while phase segregation, with cylindrical morphology, was

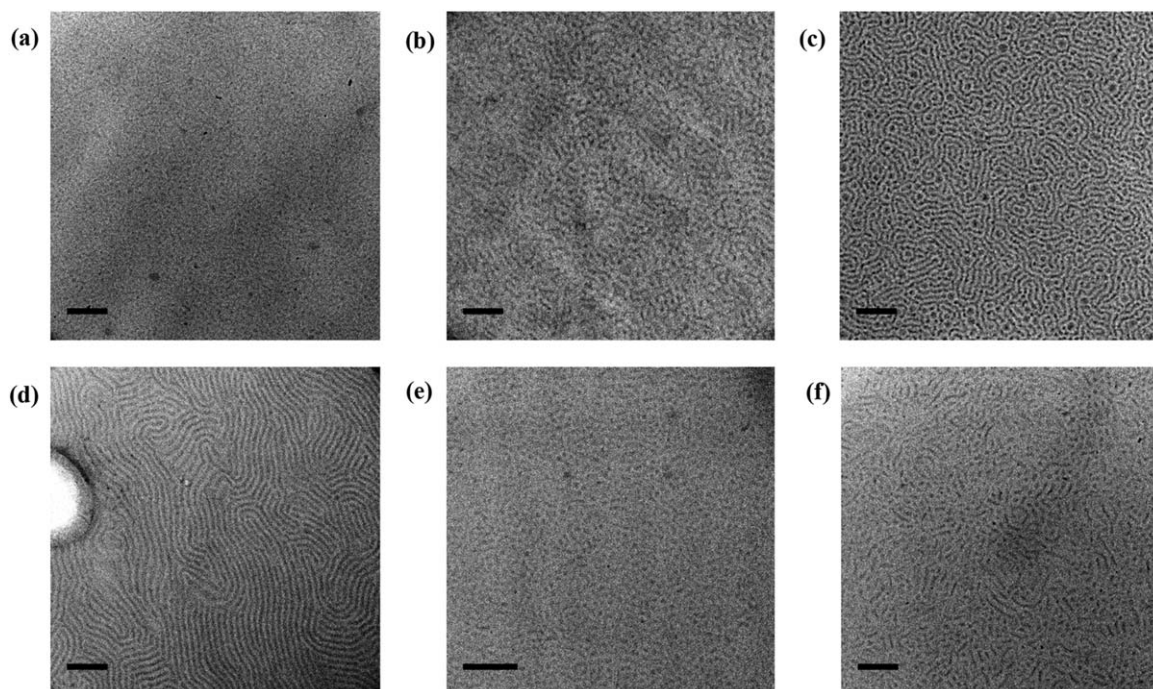


FIGURE 7 TEM bright field micrographs of: (a) PMMA-*b*-PDAP_C, (b) PMMA-*b*-PDAP_D, (c) {PMMA-*b*-PDAP_C • tAZO}, (d) {PMMA-*b*-PDAP_D • tAZO}, (e) {PMMA-*b*-PDAP_C • dAZO}, and (f) {PMMA-*b*-PDAP_D • dAZO} (the size of the black bar is 200 nm).

observed in Figure 7(b) for **PMMA-*b*-PDAP_D**. In the supramolecular block copolymers, the incorporation of H-bonded azoderivates into the PDAP domains of the parent diblock copolymers alters their original morphology because of a change in the composition (Table 2). TEM images show a cylindrical morphology for **{PMMA-*b*-PDAP_C • tAZO}** [Fig. 7(c)] while a lamellar one seems to be observed for **{PMMA-*b*-PDAP_D • tAZO}** [Fig. 7(d)]. In the case of supramolecular block copolymers with **dAZO**, block copolymer **{PMMA-*b*-PDAP_C • dAZO}** did not show a clear and well-defined morphology [Fig. 7(e)], although a lamellar one was expected according to its composition, meanwhile **{PMMA-*b*-PDAP_D • dAZO}** seems to be cylindrical [Fig. 7(f)].

Optical Properties and Photoinduced Optical Anisotropy

The optical absorption, as well as the photoinduced birefringence (Δn) and dichroism of the four supramolecular block copolymers have been investigated. The results were different for **dAZO** and **tAZO** containing supramolecular polymers but similar within each family, once normalized to the same azo content. Because of this, only the results corresponding to **{PMMA-*b*-PDAP_C • dAZO}** and **{PMMA-*b*-PDAP_C • tAZO}** will be reported as representative examples of each family.

Films for optical studies (0.5–1 μm thick) were prepared by casting dichloromethane solutions of the supramolecular complexes onto glass substrates. Prior to perform optical measurements, films were annealed in air at 150 °C for 5 min and rapidly quenched to RT.

UV-vis absorption spectra of the films after thermal treatment are given in Supporting Information (Fig. S11). They showed a strong band with a peak in the 355–365 nm region, together with a shoulder at about 450 nm. These absorptions correspond to the π - π^* and n - π^* transitions of the *trans* azo moiety, respectively. The width of the UV band is higher in the dAZO copolymers than in the tAZO ones. Besides, the band position in dAZOs appears at higher energy than in tAZOs. This can be associated with the presence of azobenzene H aggregates that are favored in the dAZO due to its dendrimeric structure.

$|\Delta n|$ values were obtained following the procedure described elsewhere.²⁹ Linearly polarized light (488 nm, 750 mW cm^{-2}) was used to induce anisotropy. In order to compare samples with different azo content we have calculated the normalized birefringence, $|\Delta n|_{\text{norm}}$ (values given in Table 2), by dividing $|\Delta n|$ by the content of azochromophore (only considering the 4-oxy-4'-cyanoazobenzene unit) in the complexes. The time evolution of $|\Delta n|_{\text{norm}}$ with irradiation time is given in Figure 8. Films were first irradiated for 60 min with the 488 nm light. This light was switched off for other 30 min.

For complexes containing **tAZO**, $|\Delta n|$ increased initially until saturation (in about 5 min) and kept the same value for longer irradiation times (up to 60 min) and then, when the 488 nm light was switched off, $|\Delta n|$ decreased. A final stable value of about 70% of the maximum one was reached. The

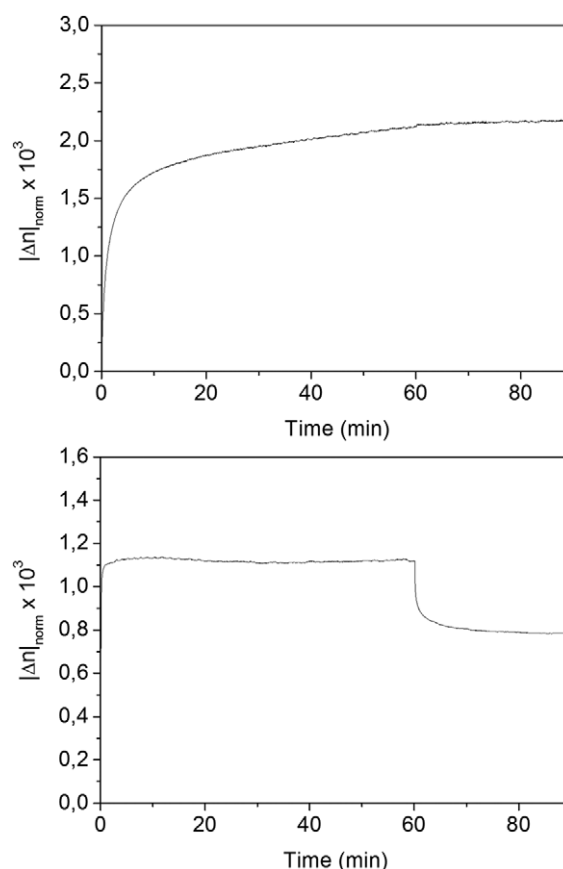


FIGURE 8 Time evolution of the normalized birefringence of the block copolymers **{PMMA-*b*-PDAP_C • dAZO}** (top) and **{PMMA-*b*-PDAP_C • tAZO}** (bottom) under irradiation with linearly polarized 488 nm light. Exciting light was switched off at 60 min.

final value of $|\Delta n|_{\text{norm}}$ was about 0.8×10^{-3} for these two copolymers.

For complexes with **dAZO**, $|\Delta n|$ also showed a fast increase in the first 5 min and then it continued growing more slowly without reaching a saturation value (in 60 min), even when increasing the irradiation time (up to 140 min) or the energy density (up to 2W cm^{-2}). In this case, when the 488 nm light was switched off $|\Delta n|_{\text{norm}}$ did not decrease (even a slow increase was observed in some of the measurements) reaching values up of $|\Delta n|_{\text{norm}}$ up to 2.1×10^{-3} .

The different time evolution and final values of photoinduced $|\Delta n|_{\text{norm}}$ in the two types of polymers can be understood taking into account the liquid crystalline behavior of polymers containing the dendrimeric **dAZO** moieties in contrast to amorphous polymers containing **tAZO**. It is known that the interactions of azo moieties in liquid crystal polymers generally improve both the photoinduced response and its stability.

Dichroism measurements have also been performed in the block copolymers. The polarized optical absorption of

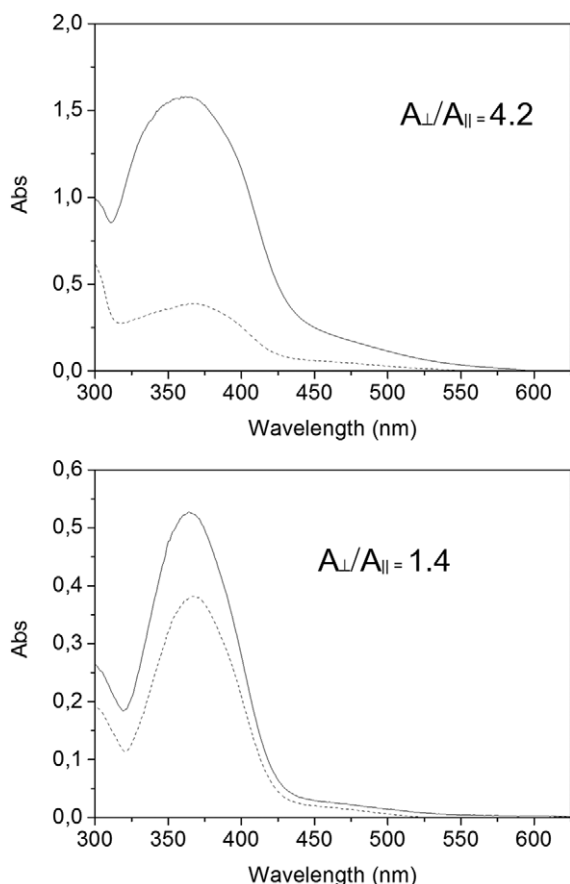


FIGURE 9 Polarized absorption spectra, of the {PMMA-*b*-PDAP_C • dAZO} (top) and {PMMA-*b*-PDAP_C • tAZO} (bottom) copolymers, after irradiation with linearly polarized 488 nm light for 60 min: parallel (dashed line) and perpendicular (continuous).

{PMMA-*b*-PDAP_C • dAZO} and {PMMA-*b*-PDAP_C • tAZO} have been measured after birefringence experiments. The results are given in Figure 9. We defined the dichroic ratio as A_{\perp}/A_{\parallel} where A_{\perp} and A_{\parallel} are the optical absorptions in the maximum of the main band measured with light linearly polarized in the direction perpendicular and parallel to the polarization of the exciting 488 nm light, respectively. The values obtained for this dichroic ratio are about 4.2 and 1.4 for {PMMA-*b*-PDAP_C • dAZO} and {PMMA-*b*-PDAP_C • tAZO}, respectively. These results are in agreement with those of $|\Delta n|_{\text{norm}}$ measurements showing that photoinduced optical anisotropy is bigger in the dAZO polymers than in the tAZO ones. It should be pointed out that dichroic ratios obtained in these materials are, in general, higher than those previously obtained in our lab for some covalent azo-containing polymers.^{27–32}

CONCLUSIONS

A new methacrylic monomer containing a moiety able to complex functional molecules via multiple H-bonding, has been easily synthesized in two synthetic steps. This monomer was polymerized via RAFT polymerization to achieve homo and copolymers with a good control of the molecular

weight and having DAP pendant groups, which were fully complexed with azobenzene chromophores having thymine or carboxyl complementary groups. The spectroscopic study of these materials reveals that the supramolecular polymers behave as homogenous materials, although a previous thermal annealing at the isotropic state is needed in case of polymers complexed with dAZO chromophores. The photoorientational properties of these materials are similar to other azobenzene covalent polymers. Thus it can be concluded that this synthetic methodology is an effective and easy approach to obtain photoaddressable polymers and avoids the time-consuming procedures associated to the preparation of azo monomers, as well as the synthetic problems found in the radical polymerization of azo (meth)acrylic monomers.^{54,55}

ACKNOWLEDGMENTS

This work was supported by the MINECO, Spain, under the project MAT2011–27978-C02-01 and –02, Fondo Europeo de Desarrollo Regional (FEDER), Gobierno de Aragón and Fondo Social Europeo. Authors would also like to acknowledge the Advanced Microscopy Laboratory and Servicio de Microscopia Electrónica de Materiales of the Universidad de Zaragoza (Servicios de Apoyo a la Investigación, SAI). I. Díez acknowledges funding from CSIC and Fondo Social Europeo through a JAE-Doc fellowship.

REFERENCES AND NOTES

- 1 J. M. Lehn, *Angew. Chem. Int. Ed.* **1990**, *29*, 1304–1319.
- 2 G. M. Whitesides, J. P. Mathias, C. T. Seto, *Science* **1991**, *254*, 1312–1319.
- 3 D. Philp, J. F. Stoddart, *Angew. Chem. Int. Ed.* **1996**, *35*, 1154–1196.
- 4 F. J. M. Hoeben, P. Jonkheijm, E. W. Meijer, A. P. H. J. Schenning, *Chem. Rev.* **2005**, *105*, 1491–1546.
- 5 T. Kato, N. Mizoshita, K. Kishimoto, *Angew. Chem. Int. Ed.* **2006**, *45*, 38–68.
- 6 L. J. Prins, D. N. Reinhoudt, P. Timmerman, *Angew. Chem. Int. Ed.* **2001**, *40*, 2382–2426.
- 7 D. J. Broer, C. M. W. Bastiaansen, M. G. Debije, A. P. H. J. Schenning, *Angew. Chem. Int. Ed.* **2012**, *51*, 7102–7109.
- 8 T. Kato, J. M. J. Fréchet, *Macromolecules* **1989**, *22*, 3818–3819.
- 9 C. Fouquey, J. M. Lehn, A. M. Levelut, *Adv. Mater.* **1990**, *2*, 254–257.
- 10 L. Brunsveld, B. J. B. Folmer, E. W. Meijer, R. P. Sijbesma, *Chem. Rev.* **2001**, *101*, 4071–4097.
- 11 J. D. Fox, S. J. Rowan, *Macromolecules* **2009**, *42*, 6823–6835.
- 12 T. Kato, M. Nakano, T. Moteki, T. Uryu, S. Ujiie, *Macromolecules* **1995**, *28*, 8875–8876.
- 13 M. Millaruelo, L. S. Chinelatto, L. Oriol, M. Piñol, J. L. Serrano, R. M. Tejedor, *Macromol. Chem. Phys.* **2006**, *207*, 2112–2120.
- 14 F. Vera, C. Almuzara, I. Orera, J. Barberá, L. Oriol, J. L. Serrano, T. Sierra, *J. Polym. Sci. Part A: Polym. Chem.* **2008**, *46*, 5528–5541.

- 15 P. Bai, M. I. Kim, T. Xu, *Macromolecules* **2013**, *46*, 5531–5537.
- 16 T. Ikeda, J.-i. Mamiya, Y. Yu, *Angew. Chem. Int. Ed.* **2007**, *46*, 506–528.
- 17 T. Ikeda, T. Ube, *Mater. Today* **2011**, *14*, 480–487.
- 18 S. Hvilsted, C. Sánchez, R. Alcalá, *J. Mater. Chem.* **2009**, *19*, 6641–6648.
- 19 R. Hagen, T. Bieringer, *Adv. Mater.* **2001**, *13*, 1805–1810.
- 20 F. K. Bruder, R. Hagen, T. Roelle, M. S. Weiser, T. Faecke, *Angew. Chem. Int. Ed.* **2011**, *50*, 4552–4573.
- 21 R. M. Tejedor, L. Oriol, J. L. Serrano, T. Sierra, *J. Mater. Chem.* **2008**, *18*, 2899–2908.
- 22 D. Liu, D. J. Broer, *Angew. Chem. Int. Ed.* **2014**, *53*, 4542–4546.
- 23 E. Blasco, M. Piñol, L. Oriol, B. V. K. J. Schmidt, A. Welle, V. Trouillet, M. Bruns, C. Barner-Kowollik, *Adv. Funct. Mater.* **2013**, *23*, 4011–4019.
- 24 E. Blasco, M. Piñol, L. Oriol, *Macromol. Rapid Commun.* **2014**, *35*, 1090–1115.
- 25 A. Natansohn, P. Rochon, *Chem. Rev.* **2002**, *102*, 4139–4175.
- 26 A. S. Matharu, S. Jeeva, P. S. Ramanujam, *Chem. Soc. Rev.* **2007**, *36*, 1868–1880.
- 27 F. J. Rodríguez, C. Sánchez, B. Villacampa, R. Alcalá, R. Cases, M. Millaruelo, L. Oriol, *Polymer* **2004**, *45*, 2341–2348.
- 28 P. Forcén, L. Oriol, C. Sánchez, R. Alcalá, S. Hvilsted, K. Jankova, J. Loos, *J. Polym. Sci. Part A: Polym. Chem.* **2007**, *45*, 1899–1910.
- 29 S. Gimeno, P. Forcén, L. Oriol, M. Piñol, C. Sánchez, F. J. Rodríguez, R. Alcalá, K. Jankova, S. Hvilsted, *Eur. Polym. J.* **2009**, *45*, 262–271.
- 30 J. del Barrio, L. Oriol, R. Alcalá, C. Sánchez, *Macromolecules* **2009**, *42*, 5752–5760.
- 31 J. del Barrio, L. Oriol, R. Alcalá, C. Sánchez, *J. Polym. Sci. Part A: Polym. Chem.* **2010**, *48*, 1538–1550.
- 32 E. Blasco, J. del Barrio, M. Piñol, L. Oriol, C. Berges, C. Sánchez, R. Alcalá, *Polymer* **2012**, *53*, 4604–4613.
- 33 A. Sidorenko, I. Tokarev, S. Minko, M. Stamm, *J. Am. Chem. Soc.* **2003**, *125*, 12211–12216.
- 34 Q. Zhang, C. G. Bazuin, C. J. Barrett, *Chem. Mater.* **2008**, *20*, 29–31.
- 35 A. Priimagi, J. Vapaavuori, F. J. Rodríguez, C. F. J. Faul, M. T. Heino, O. Ikkala, M. Kauranen, M. Kaivola, *Chem. Mater.* **2008**, *20*, 6358–6363.
- 36 Y. Zhao, K. Thorkelsson, A. J. Mastroianni, T. Schilling, J. M. Luther, B. J. Rancatore, K. Matsunaga, H. Jinnai, Y. Wu, D. Poulsen, J. M. J. Fréchet, A. P. Alivisatos, T. Xu, *Nat. Mater.* **2009**, *8*, 979–985.
- 37 R. Fernández, H. Etxeberria, A. Eceiza, A. Tercjak, *Eur. Polym. J.* **2013**, *49*, 984–990.
- 38 J. del Barrio, E. Blasco, L. Oriol, R. Alcalá, C. Sánchez-Somolinos, *J. Polym. Sci. Part A: Polym. Chem.* **2013**, *51*, 1716–1725.
- 39 J. del Barrio, E. Blasco, C. Toprakcioglu, A. Koutsioubas, O. A. Scherman, L. Oriol, C. Sánchez-Somolinos, *Macromolecules* **2014**, *47*, 897–906.
- 40 J. F. Lutz, A. F. Thünemann, R. Nehring, *J. Polym. Sci. Part A: Polym. Chem.* **2005**, *43*, 4805–4818.
- 41 R. McHale, R. K. O'Reilly, *Macromolecules* **2012**, *45*, 7665–7675.
- 42 Y. C. Wu, S. W. Kuo, *Polym. Chem.* **2012**, *3*, 3100–3111.
- 43 R. Deans, F. Ilhan, V. M. Rotello, *Macromolecules* **1999**, *32*, 4956–4960.
- 44 F. Ilhan, T. H. Galow, M. Gray, G. Clavier, V. M. Rotello, *J. Am. Chem. Soc.* **2000**, *122*, 5895–5896.
- 45 F. Ilhan, M. Gray, V. M. Rotello, *Macromolecules* **2001**, *34*, 2597–2601.
- 46 V. Nandwana, B. Fitzpatrick, Q. Liu, K. M. Solntsev, X. Yu, G. Y. Tonga, S. Eymur, M. Tonga, G. Cooke, V. M. Rotello, *Polym. Chem.* **2012**, *3*, 3072–3076.
- 47 J. Bernstein, B. Stearns, E. Shaw, W. A. Lott, *J. Am. Chem. Soc.* **1947**, *69*, 1151–1158.
- 48 G. Moad, E. Rizzardo, S. H. Thang, *Polymer* **2008**, *49*, 1079–1131.
- 49 Y. K. Chong, T. P. T. Le, G. Moad, E. Rizzardo, S. H. Thang, *Macromolecules* **1999**, *32*, 2071–2074.
- 50 O. Ikkala, G. ten Brinke, *Chem. Commun.* **2004**, 2131–2137.
- 51 J. T. Korhonen, T. Verho, P. Rannou, O. Ikkala, *Macromolecules* **2010**, *43*, 1507–1514.
- 52 F. S. Bates, *Science* **1991**, *251*, 898–905.
- 53 M. Walther, H. Finkelmann, *Prog. Polym. Sci.* **1996**, *21*, 951–979.
- 54 O. Nuyken, R. Weidner, In *Chromatography/Foams/Copolymers*; Y. Doi, Ed.; Springer-Verlag: Berlin-Heidelberg, **1986**, Chapter 4, pp 145–199.
- 55 M. Hallensleben, B. Weichart, *Polym. Bull.* **1989**, *22*, 553–556.